THE JOURNAL OF BIOLOGICAL CHEMISTRY VOL. 287, NO. 49, pp. 41139–41151, November 30, 2012

Biochemical Characterization of P4-ATPase Mutations Identified in Patients with Progressive Familial Intrahepatic Cholestasis*

Received for publication, August 23, 2012, and in revised form, October 5, 2012 Published, JBC Papers in Press, October 11, 2012, DOI 10.1074/jbc.M112.413039

Alex Stone, Christopher Chau, Christian Eaton, Emily Foran, Mridu Kapur, Edward Prevatt, Nathan Belkin, David Kerr, Torvald Kohlin, and Patrick Williamson[1]

From the Department of Biology, Amherst College, Amherst, Massachusetts 01002

Background: Mutations in the P4-ATPase ATP8B1 cause progressive familial intrahepatic cholestasis (PFIC).
Results: Homologous mutations in yeast P4-ATPase Dnf2p alter enzyme activity and subunit interaction phenotypes.
Conclusion: This approach provides a method for characterizing the pathological basis of PFIC mutations.
Significance: This approach identifies residues involved in substrate binding and a potential path for phospholipid movement.

Mutations in the P4-ATPase ATP8B1 cause the inherited liver disease progressive familial intrahepatic cholestasis. Several of these mutations are located in conserved regions of the transmembrane domain associated with substrate binding and transport. Assays for P4-ATPase-mediated transport in living yeast cells were developed and used to characterize the specificity and kinetic parameters of this transport. Progressive familial intrahepatic cholestasis mutations were introduced into the yeast plasma membrane P4-ATPase Dnf2p, and the effect of these mutations on its catalysis of phospholipid transport were determined. The results of these measurements have implications for the basis of the disease and for the mechanism of phospholipid transit through the enzyme during the reaction cycle.

P4-ATPases are a subfamily of the ATP-dependent P-type ATPases; members of this subfamily have been shown to catalyze transbilayer transport of phospholipids (1–3). P4-ATPases couple ATP hydrolysis to the transport of phospholipids from the outer or lumenal leaflet to the cytoplasmic leaflet of membranes and are found in eukaryotes but not prokaryotes (4). Most of the members of this subfamily of transporters operate as heterodimers in combination with subunits from the Cdc50 family of membrane proteins (5); both proper localization and transport activity require transporter association with the subunit (6–8).

In humans, there are 14 genes for P4-ATPases. Mutations in one of them, ATP8B1 or FIC1, give rise to the rare autosomal recessive diseases progressive familial intrahepatic cholestasis (PFIC1[2] or Byler disease) and the related but less severe benign recurrent intrahepatic cholestasis (BRIC1) (9). The disease results in defects in bile salt secretion in the liver canaliculi, leading to episodes of jaundice and severe pruritus, together with nonhepatic symptoms that can include growth defects, diarrhea, and hearing loss; expressivity of the mutations is often variable (10). The protein product of this gene appears in the apical membranes of a variety of epithelia and notably in the canalicular membrane of the liver (11) and the stereocilia membrane in hair cells (12).

Analysis of PFIC and BRIC patients have identified a significant range of ATP8B1 mutations that give rise to the disease (10). As might be expected, PFIC patients harbor more severe changes in the gene, such as frameshift and nonsense mutations, whereas BRIC is more generally associated with single missense mutations that may result in residual enzyme activity (10). Missense mutations occur throughout the protein sequence but can be roughly assigned to two locations, cytoplasm and membrane, based on their position in the sequence and the overall conservation of this sequence in the P-type ATPase family. The structure of P-type ATPases (13) includes a large, highly conserved cytoplasmic region organized into the phosphorylation (*P*), nucleotide binding (*N*), and actuator (*A*) domains (see Fig. 3). These domains cooperate to bind ATP, phosphorylate the critical Asp in the phosphorylation domain, release ADP, and then hydrolyze the aspartylphosphate. Many of the PFIC and BRIC mutations occur in one of these cytoplasmic domains and can therefore be expected to interfere with this well understood sequence of steps that makes up the ATP hydrolysis reaction. More problematical (and more specific to the P4 subfamily) are mutations that alter amino acids in the membrane region, because this region determines the specificity of substrate transport and is also a potential locus of interaction with the subunit, itself a transmembrane protein. It is therefore likely that study of the phenotype of these mutants can shed light on these aspects of P4-ATPase transport.

However interesting these phenotypes might be, they cannot be easily studied in ATP8B1 for several reasons. First, it is not clear what phospholipids this mammalian enzyme transports. Based on the phospholipid composition of bile (14) and on accumulation of fluorescent phospholipids in transfected cells

* This work was supported in part by National Science Foundation Grant 0443858 (to P. W.), by a Howard Hughes Medical Institute Grant (to Amherst College), and by a Faculty Research Grant from Amherst College.
[1] To whom correspondence should be addressed: Dept. of Biology, Amherst College, McGuire Life Science Bldg., Amherst, MA 01002. Tel.: 413-542-2143; E-mail: plwilliamson@amherst.edu.
[2] The abbreviations used are: PFIC, progressive familial intrahepatic cholestasis; BRIC, benign recurrent intrahepatic cholestasis; NBD, 1-acyl-2-(6-((7-nitro-2–1,3-benzoxadiazol-4-yl)amino)hexanoyl)-*sn*-glycero-3-phospho; PS, phosphatidylserine; PC, phosphatidylcholine; HBS, Hanks' buffered saline; Cub, C-terminal fragment of ubiquitin; Nub, N-terminal fragment of ubiquitin.

TABLE 1
Yeast strains used in this study

Name	Genotype	Source
PFY3275F	*MATa his3, Leu2, Ura3, met15, dnf1Δ, dnf2Δ*	Ref. 18
SEY6210	*MATα leu2-3112 ura3-52 his3-200*	Ref. 50
JMY749	Diploid *his3-A200 leu2-A1 ura3-52 lys2-801 trp -Al 01*	Ref. 51
THYAP5	*MATα lexA-ADE2 leu2 trp1 his3*	Ref. 29
THYAP4	*MATa lexA-lacZ-TRP1 lexA-HIS3 lexA-ADE2 ura3 leu2*	Ref. 29
TPY051	*MATa leu2-3, trp1-901, his3-Δ200, ade2-101*	Ref. 20
TPY053	*MATa leu2-3, trp1-901, his3-Δ200, ade2-101, dnf2Δ*	Ref. 20
TPY055	*MATa leu2-3, trp1-901, his3-200, ade2-101, dnf1Δ*	Ref. 20
TPY058	*MATa leu2-3, trp1-901, his3-200, ade2-101, dnf1Δ, dnf2Δ*	Ref. 20
TPY066	*MATa leu2-3, trp1-901, his3-200, ade2-101, dnf1Δ, dnf2Δ, Δdrs2*	Ref. 20

(15), it has been suggested that the enzyme transports phosphatidylserine (PS) to the cytoplasmic leaflet from the cell surface. However, small RNAi inhibition of ATP8B1 expression has been reported to have no effect on PS transport in Caco-2 cells (16). Second, it is not clear where the transport takes place; ATP8B1 is related to the ATP8A1/Drs2p class of P4-ATPases that play an important role in intracellular vesicle trafficking (17, 18). Third, it has been suggested that ATP8B1 interacts with two different subunits, CDC50A and CDC50B, (15, 19), but the latter may not be entirely functional (19).

Fortunately, understanding the biochemical phenotype of these mutations is not necessarily limited by these issues with ATP8B1 because the mutations themselves are largely in residues that are conserved across the P4-ATPase subfamily. It is therefore possible to consider measuring the impact of these mutations in a biochemically more tractable system. Ideally, such a system should have 1) a P4-ATPase with well characterized transporter activity and specificity, 2) well characterized subunit interactions, and 3) robust assays for measuring changes in these characteristics. For this purpose, we turned to *Saccharomyces cerevisiae*, which has five P4-ATPases. Two of these, Dnf1p and Dnf2p, are plasma membrane enzymes (20) that internalize phosphatidylcholine (PC) from the outer leaflet of the plasma membrane. The subunit from the Cdc50 family that interacts with these enzymes (Lem3p) is well known, and there is already a sensitive assay based on the split ubiquitin system for assessing this interaction (6). Low resolution assays for measuring phospholipid transport in yeast have been reported (20–23), but a higher resolution assay capable of measuring enzyme kinetic parameters was developed here to complement the subunit interaction assay. These assays make it possible to assess the biochemical consequences of introducing the mutations identified in PFIC/BRIC patients into a yeast transporter. The development and application of the transport assay and the results of the characterization of such mutants are reported here.

EXPERIMENTAL PROCEDURES

Reagents—Unlabeled and NBD labeled ((1-acyl-2-(6-((7-nitro-2-1,3-benzoxydiazo-4-yl)amino)-hexanoyl)-*sn*-glycero-3-phosphocholine were purchased from Avanti Polar Lipids. Zymolase (20,000 units/g) was obtained from MP Biochemicals LLC. β-Glucuronidase (112,400 units/ml) was obtained from Sigma-Aldrich. AlexaFluor 488-labeled monoclonal antibody HA-11 to the HA tag was obtained from Covance (catalogue number A488-101L). Pierce Y-PER yeast permeabilization reagent was obtained from Thermo Scientific. *O*-Nitrophenyl-β-D-galactopyranoside was obtained from Sigma-Aldrich.

Plasmids and Yeast Strains—The *dnf2* gene cloned into pRS426 as described previously for *drs2* (6) was a gift of Joost Holthuis (University of Utrecht). pMetYC-gate, pNubWT-Xgate, and pNXgate33–3HA were provided by Christopher Grefen (University of Tubingen).

PFY3275 and SEY6210 were provided by Ryan Baldridge and Todd Graham (Vanderbilt University). TPY051, TPY053, TPY055, TPY058, and TPY066 were provided by Thomas Pomorski and Joost Holthuis (University of Utrecht). THY AP4 and THY AP5 were provided by Christopher Grefen (University of Tubingen). A complete list of yeast strains used is provided in Table 1.

Mutant Generation—To mutagenize *dnf2*, fragments harboring the desired base changes were generated by PCR and inserted into gapped parental pRS426-*dnf2* (24) by *in vivo* recombination in the Δ*dnf1*/Δ*dnf2* strain PFY3275 (25). Primers for the mutagenesis are listed in Table 2. For analysis by the mating-based split ubiquitin method, mutated *dnf2* genes were tagged with B1 and B2 sequences by PCR and introduced into the pMetYCgate vector (26, 27) in ThyAP4 yeast. Primers for the tagging of B1 and B2 to *dnf2* were identical to those used in previous studies (6). Successful mutant construction was confirmed by sequencing.

NBD Phospholipid Transport—The rate of NBD-labeled phospholipid uptake was measured in a Beckman Coulter XL EPICS flow cytometer. Yeast was taken from cultures in log phase growth after dilution of at least 1:100 from overnight into selective medium. For measuring the effects of methionine levels on the activity of Dnf1p expressed from a methionine promoter, yeast grown overnight in the absence of methionine was diluted into medium containing 0.01 or 0.3 mM methionine and grown until they reached log phase. In all cases, cells were collected by centrifugation and diluted in Hanks' buffered saline (HBS) to a concentration yielding about 500 events/s in the cytometer. Propidium iodide (Sigma-Aldrich) was added to this suspension to label dead cells. An aliquot of NBD-labeled phospholipid dissolved at 1 mg/ml in chloroform was dried under a stream of argon and resuspended at a concentration of 40 μg/ml in HBS. Aliquots of this micellar suspension were diluted into the yeast suspension to the desired final concentration, and the mixture was introduced into the cytometer. The time from the addition of probe to the onset of data collection was 15 ± 2 s; this "dead time" limits the resolution of measurements of

TABLE 2
Primers used for site-directed mutagenesis of *dnf2*

Mutation	Primer	Sequence
L264P	Mutating	5′-CTTTTTAATAC**C**GTTGATTCTAG-3′
	Forward (SpeI)	5′-AACAATATGAATTCCTGCAGCCCGGG-3′
	Reverse (EcoNI)	5′-GTTCCTCTTCCTTCGTAATTCTTCCC-3′
N601F	Mutating	5′-CTGTGATTTTG**TT**TTTTGTACTATTG-3′
	Forward (EcoNI)	5′-GCTTACCGTTGGCAGTTTAC-3′
	Reverse (BsrGI)	5′-CACGTCCATAAGACACACCGTT-3′
K670P	Mutating	5′-CTGTGGAAATTATT**CC**GACAGCACAGGC-3′
	Forward (EcoNI)	5′-GCTTACCGTTGGCAGTTTAC-3′
	Reverse (BsrGI)	5′-CACGTCCATAAGACACACCGTT-3′
E1251K	Mutating	5′-GTACGTATACT**T**AAACAAATACGACC-3′
	Forward (MscI)	5′-GCAGTGGTCAAGTTGGTAAA-3′
	Reverse (SacII)	5′-CGATCCAGCGAAGTTCTGAGC-3′
G1320R	Mutating	5′-CATGTTGGAT**CGT**GTATACCAATC-3′
	Forward (AccIII)	5′-GTCGAATCGGAAGGTCGTC-3′
	Reverse (SacII)	5′-CGATCCAGCGAAGTTCTGAGC-3′

very fast fluorescence changes. Substrate specificity experiments were conducted using saturating probe concentrations.

Data were analyzed using WinMDI2.9 (Joe Trotter, The Scripps Research Institute). Cells with high binding of propidium iodide were gated out, and cells of a restricted size class (corresponding roughly to gate 3 in Fig. 1*A*) were selected. In the data for the cells transformed with pRS426/*dnf2* and its mutants, a variable fraction of the cells were not transporting at all; the kinetic data presented here are only for those cells that were engaged in transport. The green (FITC) fluorescence from the gated cells actively engaged in transport was collected in logarithmic mode, and the resulting data set was analyzed using SigmaPlot (Systat Software, Inc.). After averaging the fluorescence intensity of all of the cells in each individual time bin (usually about 0.6 s), the data were smoothed by averaging 5–10 s of data, and the rate of fluorescence increase was determined by linear regression. Kinetic parameters were determined from such rates by nonlinear regression to the Michaelis-Menten equation. Apparent V_{max} values for mutants were determined in comparison with values for the wild type determined in parallel on each day to control for cytometer variation. Averages for kinetic parameters were made from measurements taken on different cultures on different days. Inhibition constants were estimated by non-linear regression to the control V_{max} at variable inhibitor concentrations (28).

Protein Expression—Yeast was inoculated from an overnight into 5 ml of selective medium and allowed to grow to log phase. After testing for transport, 2 ml of cells were spun down gently, washed with HBS, and then fixed with 2% paraformaldehyde in HBS at room temperature for 10 min. The paraformaldehyde was quenched and removed by washing with HBS containing 1 M glycine, and the cells were then resuspended in 1 ml of HBS plus 1 M sorbitol and converted to spheroplasts by adding 10 units of zymolase and 50 units of β-glucuronidase and incubating for 15 min at room temperature. Fifty μl of this suspension of spheroplasts was centrifuged and resuspended in 15 μl of HBS plus 1 M sorbitol containing 1% Triton X-100. Five μl of a 1:200 dilution in HBS of AlexaFluor-labeled anti HA antibody was added, and the mixture was incubated for 30 min at room temperature. The mixture was then diluted 50-fold with HBS plus 1 M sorbitol, propidium iodide was added, and the cells were introduced into the cytometer. Fluorescence was measured in the green (FITC) channel for those cells that were propidium iodide-positive. There was no green fluorescence above that of the negative control under these conditions for cells in the population that could still exclude propidium iodide.

Transporter-Subunit Interaction—Interaction of mutated Dnf2p transporters with Lem3p was assessed using the mating-based split ubiquitin assay as described previously (6, 29). Briefly, the transporter was tagged at the C terminus with the C-terminal fragment of ubiquitin (Cub) followed by the LexA reporter and expressed in the ThyAP4 MATa strain of yeast. Lem3p was tagged at the N terminus with the N-terminal fragment of ubiquitin (Nub) and expressed in the ThyAP5 MATα strain of yeast. ThyAP5 cells transformed with pNubWT-Xgate and overexpressing a Nub fragment capable of spontaneous interaction with the Cub tag provided a positive control for Cub expression, whereas ThyAP5 cells containing an empty Nub vector, pNXgate33-3HA, provided a negative control for background Cub activity. To assay interaction, *dnf2*-Cub and Nub strains were cocultured on rich medium plates to allow mating, and diploids were then selected by replica plating on selective medium lacking leucine and tryptophan and containing methionine. Interaction was assessed by a preliminary growth assay carried out by replicating these plates onto similar plates lacking adenine and histidine. For the quantitative measurements of interaction, 1 ml of log phase cultures of diploids in liquid medium lacking adenine, tryptophan, and methionine were collected, washed in water, pelleted, and permeabilized in 200 μl of Y-PER reagent for 20 min at room temperature. Aliquots of this suspension were diluted into 1 ml of Z-buffer (60 mM Na_2HPO_4, 40 mM NaH_2PO_4, 10 mM KCl, 1 mM $MgSO_4$) containing 400 μg/ml *O*-nitrophenyl-β-D-galactopyranoside and incubated for 10 min at 37 °C. The reaction was stopped by the addition of 0.5 ml of 1 M sodium carbonate, the cell bodies were removed by centrifugation, and the absorbance of the supernatant was measured at 410 nm. Activity was normalized to the A_{600} of the initial culture to correct for differences in initial cell number.

Sequence Alignments—Approximately 250 fungal P4-ATPase protein sequences and 100 fungal proton transporter sequences were aligned using the Promals3D server and default settings. The *Arabidopsis thaliana* proton transporter (30) (Protein Data Bank entry 3B8C) was used as the input structure (31). The resulting alignment was trimmed of proton transporter sequences, and the conservation at each position in the P4-ATPase sequences was calculated using the Consurf server, again with default settings (32).

RESULTS

Transport of NBD-labeled Phospholipids by Living Yeast Cells—Although NBD-labeled phospholipids have often been used to measure phospholipid transport in yeast, the kinetics of this process are not well characterized. We therefore used flow

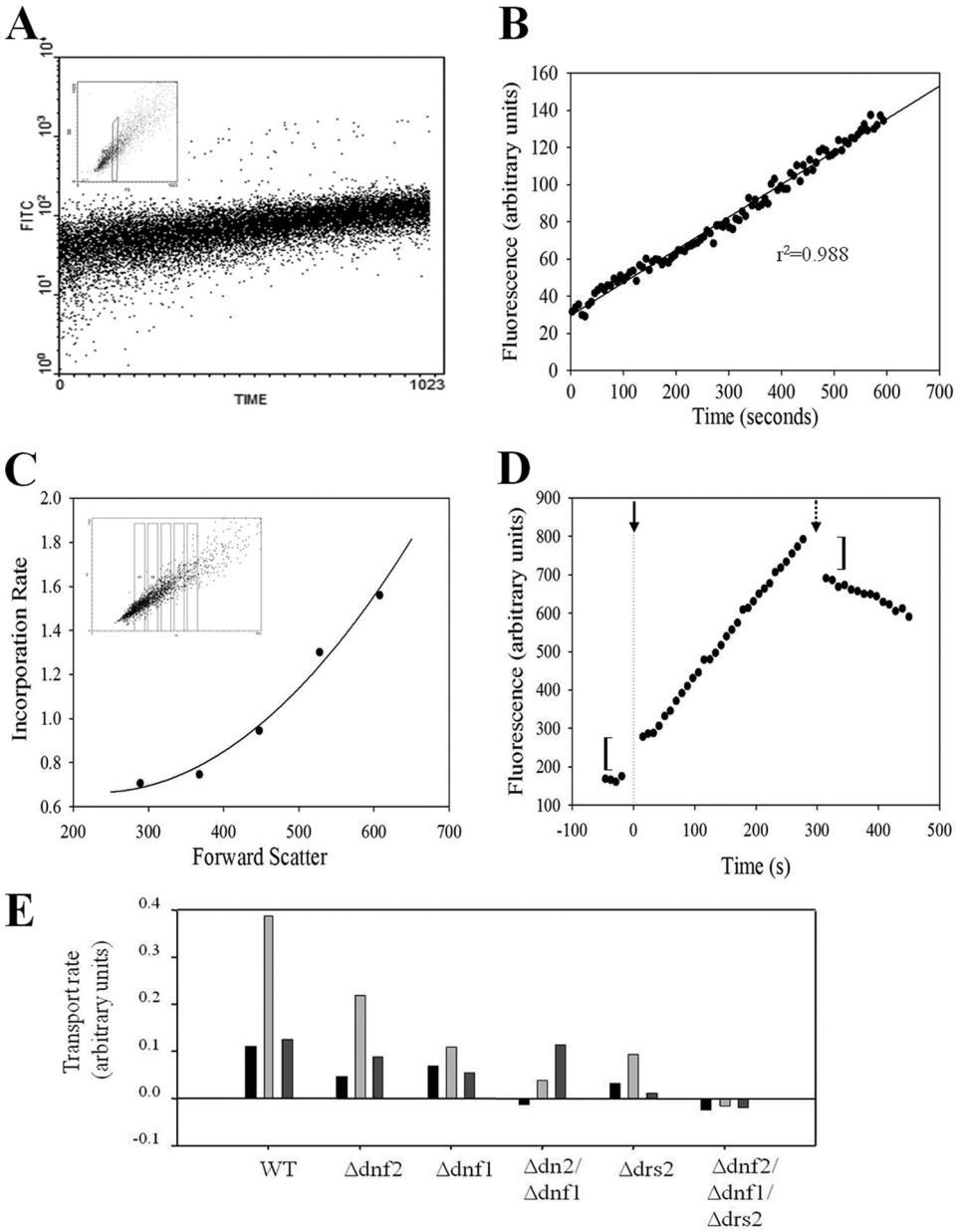

FIGURE 1. **NBD-labeled phospholipid uptake by live yeast.** *A*, dot plot of log fluorescence (FITC is on the log scale) *versus* time of wild type yeast (TPY51) treated with 1-oleoyl-NBD-PC. Only cells falling in the forward scatter gate shown in the *inset* are plotted. *B*, time course of fluorescence increase from data shown in *A* after averaging and conversion to linear fluorescence. The line shown was determined by linear regression. *C*, dependence of phospholipid uptake rate on cell size. The slope of linear regressions determined as shown in *B* are plotted against average forward scatter for the regions shown in the *inset*. *D*, dithionite quenching experiment after MPC incorporation into WT yeast (THYAP5). After an initial measurement of intrinsic fluorescence, NBD-PC was added (*solid arrow*), and data were taken. At the *dashed arrow*, the sample was removed from the cytometer, dithionite was added, and the mixture was returned to the cytometer. *Brackets* show estimates of the size of fluorescence changes that occur too quickly to be recorded. *E*, headgroup specificity of yeast phospholipid transport. The rate of transport, determined as in Fig. 1*B*, was determined for uptake of PC (*black*), PE (*light gray*), and PS (*dark gray*). *WT*, TPY51; Δ*dnf1*, TPY55; Δ*dnf2*, TPY53; Δ*dnf1*, TPY61; Δ*dnf1*/Δ*dnf2*, is TPY58; Δ*dnf1*/Δ*dnf2*/Δ*drs2*, TPY66.

cytometry to measure the fluorescence of individual yeast cells as a function of time after exposure to NBD-labeled phosphatidylcholine (NBD-PC). As shown in Fig. 1*A*, cells become steadily more fluorescent over a 10-min incubation at room temperature. To simplify the analysis, we gated for a narrow range of cell sizes (Fig. 1*A*, *inset*) and calculated the average fluorescence for those cells in consecutive time intervals. The results of this analysis, drawn on linear axes in Fig. 1*B*, show that fluorescence is increasing linearly over this time. As shown in Fig. 1*C*, the selection of an individual size fraction has an important impact on the measured rate of this fluorescence increase; larger cells are transporting more quickly (per cell), so that the rate of uptake increases monotonically with the forward scatter for each cell. For this reason, all comparisons reported here are always for cells that fall in the same forward scatter gate.

A close examination of the kinetics of this uptake (Fig. 1*D*) shows that the increased cell fluorescence actually has two components. One component can be seen by extrapolating the linear uptake back to the time of probe addition. The extrapolated intercept is reproducibly higher than the intrinsic fluores-

cence of the cells, indicating that there is a small increase in fluorescence, which is complete within the 15 s between the addition of the probe and the onset of data collection by the cytometer. The rate of this increase is thus too fast to measure. This rapid initial increase in fluorescence is then followed by the slower linear increase in fluorescence. To determine whether either of these components corresponds to probe reaching the inside of the cell, we used the membrane-impermeant reducing agent sodium dithionite. This reagent converts the nitro moiety of the NBD group to an amine and thereby reduces its fluorescence by about 100-fold; because it is an impermeant anion, it only affects probe that is not in the cell interior (33). As shown in Fig. 1*D*, the addition of this reagent after a period of incorporation produces a fast reduction in fluorescence, followed by a much slower decay. The first of these corresponds roughly in magnitude to the initial rapid rise in fluorescence observed at time 0. Its rate is dependent on the dithionite concentration and thus corresponds to reduction of probe that is cell-associated but not inside the cell. The rate of the second decay phase does not depend on dithionite concentration (data not shown), implying that the slower component corresponds to inaccessible, internalized probe reaching the external surface either by flip from the internal leaflet, by exocytosis, or by degradation to a membrane-permeable form. The possibility that these results were an artifact of dithionite treatment was tested by carrying out similar experiments without dithionite, using BSA added to the medium to extract probe that was not internal. The results observed were virtually identical to those shown here for dithionite (data not shown), indicating that these results are not peculiar to the use of dithionite. Together, these data suggest that 1) NBD phospholipid becomes associated with cells at a rate that is too fast to measure; 2) the size of this external pool of probe is very small and changes very little during the first minutes of incubation; 3) at any given time, the total cell-associated fluorescence includes both internal and external probe; and 4) the linearly increasing amount of probe corresponds to transport of the phospholipid analog into the cell interior.

In mammalian cells, phospholipid transport is restricted to internalization of PE and PS, with the rate of the latter predominating, and PC is not transported at all (34). Application of the assay described above with NBD-labeled PC, PE, and PS showed that phospholipid transport in yeast does not conform to this pattern (Fig. 1*E*). In particular, PE is generally the most rapidly transported phospholipid, whereas PC and PS are transported well and at about equal rates. In contrast to previous reports (20), we found no evidence for internalization of sphingomyelin (data not shown). Single deletions of *dnf1*, *dnf2*, or *drs2* all reduce but do not eliminate transport (Fig. 1*E*). PC transport is completely abrogated in yeast harboring deletions of both *dnf1* and *dnf2*, showing clearly that these two transporters are responsible for PC transport at the plasma membrane observed in wild type cells as well as for much of the transport of PE. In the absence of the protein products of these two genes, the remaining transport of the aminophospholipids PS and PE resembles that seen in mammalian cells. Finally, the data show that further deletion of *drs2* eliminates transport of all phospholipid types, implying that the other two P4-ATPases, Neo1p and Dnf3p, play no role at all in phospholipid transport at the yeast plasma membrane. Single deletion of *dnf3* has no effect on transport, confirming this conclusion. The effect of deletion of *neo1* on transport cannot be tested, because deletions of this P4-ATPase are lethal.

These observations suggest that, properly applied, these measurements could provide a quantitative assay for enzyme-catalyzed active transport of phospholipids. To test whether the rate of transport is dependent on the amount of transporter present in the membrane, we took advantage of the fact that, in the absence of Dnf2p, internalization of NBD-PC is completely dependent on Dnf1p. We therefore introduced a plasmid containing the *dnf1* gene under the control of a methionine promoter into a Δ*dnf1*/Δ*dnf2* double deletion strain. As shown in Fig. 2*A*, the rate of transport for NBD-PC in this system is now regulated by the level of methionine in the medium, implying that the transport rate is a function of the amount of transporter in the cell. Second, we tested whether the rate of transport is dependent on substrate concentration in a saturable manner. To this end, we measured the rate of transport with NBD-labeled phospholipid presented to the cells in the absence of carrier vesicles or detergent micelles that present nonsaturable, competing binding sites for the probe. As shown in Fig. 2*B*, Under these circumstances, the rate of transport is substrate concentration-dependent and is saturable. One important consideration is that the free probe concentration is limited by the critical micelle concentration of the probe, and we therefore compared the concentration dependence using NBD-PC with either oleoyl or myristoyl side chains in the C1 position of the glycerol backbone; the critical micelle concentration of these two versions of the probe should differ by about a factor of 40 (35). As shown in Fig. 2*B*, the dependence of the rate of transport on probe concentration is the same in both cases, showing that 1) transport rate is dependent on saturable binding of phospholipid to an external binding site, 2) this dependence is not an artifact of probe critical micelle concentration, and 3) the affinity of the transporter for the probe is not very sensitive to small changes in fatty acid side chain length.

The ability to make quantitative estimates of transporter activity in yeast facilitated investigation of two basic cell biological questions about transport. The first question is whether phospholipid transport rates change depending on whether the cell is dividing. To examine this question, we inoculated yeast from a stationary culture into fresh medium and measured transport rates at intervals after inoculation. As shown in Fig. 2*C*, stationary phase yeast barely transports at all. As the yeast enters into logarithmic phase growth, transport rates increase, reaching a plateau by about 3 h after inoculation. Comparison of transport rates with probes containing different headgroups and yeast containing different deletions showed a similar pattern for all major phospholipid groups and all three transporters (data not shown). Because of this finding, care was taken to ensure that cells were well into log phase growth when they were taken for transport measurements.

A quantitative assay for phospholipid internalization rate in yeast also provides a platform for investigating interactions with substrates for which suitable fluorescent versions are not available. For example, it has been suggested that the P4-ATPases are

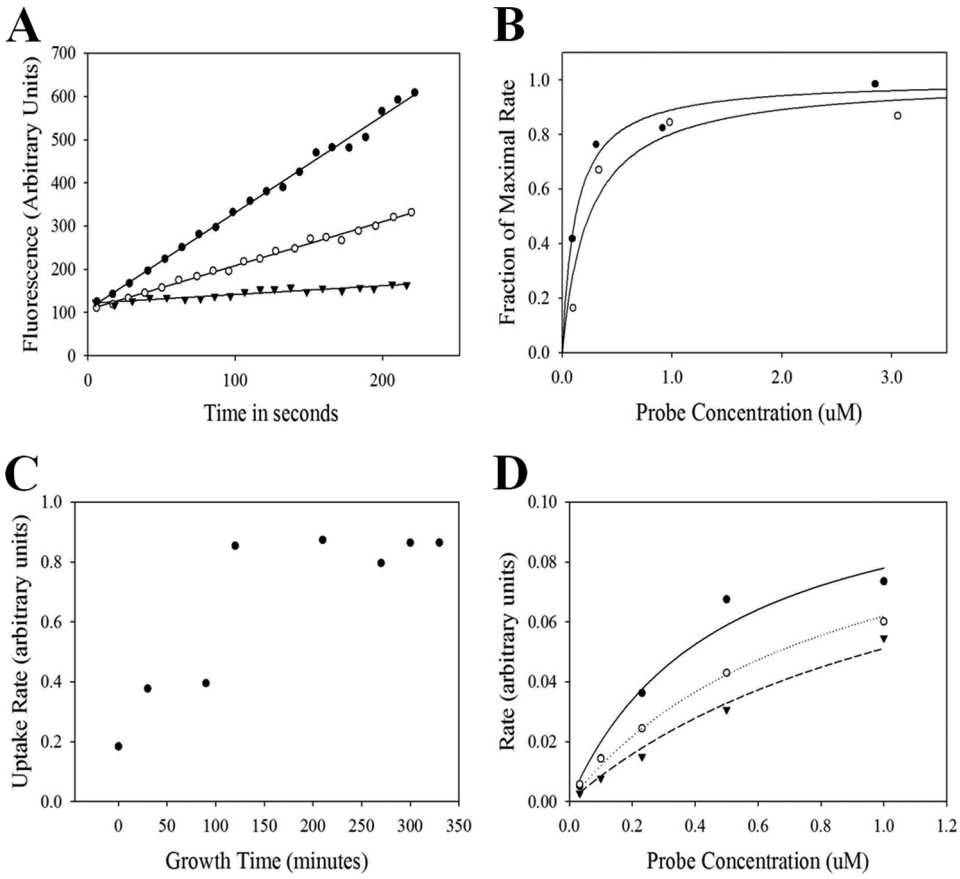

FIGURE 2. **Characteristics of NBD-PC uptake.** *A*, transport rate is dependent on level of transporter expression. Δ*dnf1*/Δ*dnf2* yeast (pFY3274F) was transformed with *dnf1* in the pMetYCgate vector and grown to log phase in SD−Leu. The increase in fluorescence in the presence of NBD-PC probe *versus* time is shown. *Filled circles*, 0.01 mM methionine; *open circles*, 0.3 mM methionine; *filled triangles*, empty vector control. *B*, NBP-PC concentration dependence of transport rate. WT yeast (SEY6210) was incubated with the indicated concentrations of NBD-PC. *Filled circles*, 1-oleoyl 2-NBD PC; *open circles*, 1-myristyrl 2-NBD PC to the transporter. *C*, change in phospholipid uptake with growth. Stationary phase wild type yeast (JM749) was diluted into fresh medium at zero time, and samples were taken for measurement of the NBD-PS uptake rate. The time on the *x* axis represents the time after dilution. *D*, wild type yeast (SEY6210) was treated with various concentrations of probe in the presence and absence of unlabeled lyso-PC (*LPC*). *Filled circles*, no lyso-PC; *open circles*, 0.1 μM lyso-PC; *filled triangles*, 0.26 μM lyso-PC.

nutrient uptake enzymes that transport lysophospholipids (36), although commercially available NBD-lyso-PC itself is not a substrate for transport in yeast (data not shown). Nevertheless, the affinity of unlabeled lysophospholipids can be measured indirectly by competition with NBD-labeled phospholipids. As shown in Fig. 2*D*, lyso-PC competes effectively with NBD-PC for binding to Dnf2p, with an apparent K_i for the lysophospholipid that was about 3-fold lower in this experiment than the apparent K_m for phospholipid. These data show that Dnf2p has a relatively strong binding affinity for a phospholipid with only one fatty acid side chain. It also suggests caution when measuring phospholipid uptake in medium that may contain such lysophospholipids.

PFIC/BRIC Mutations in dnf2—As shown above, Dnf1p and Dnf2p are the primary transporters of PC at the yeast plasma membrane, and uptake of PC can be used to specifically characterize this transport after reintroduction of one of these transporters into a double deletion strain. Indeed, these properties have already been used to study the effects of mutations on transporter specificity (25). With the quantitative assay described above, it is possible to obtain information on maximum transport rates and substrate affinity of such reintroduced transporters, which can be combined with measurements of transporter/subunit interaction using the split ubiquitin assay. PFIC/BRIC mutations affecting residues in the transmembrane region, as shown in Fig. 3*A*, were selected for study because of the likelihood that the phenotype of these mutations would reflect changes in substrate/transporter properties. The chosen PFIC/BRIC residues are generally well conserved across P4-ATPases (Fig. 3*B*), making it likely that these mutations, which clearly have phenotypic consequences when they occur in ATP8B1, will have similar consequences when introduced into Dnf2p.

G1320R—The G1040R mutation in ATP8B1, corresponding to a G1320R mutation in Dnf2p, was identified in a Saudi patient (10). It replaces a reasonably conserved glycine with a charged arginine in the middle of a transmembrane helix (TM7) and thus might be expected to destabilize the protein, although, as shown in Fig. 3*B*, the P4-ATPases have relatively hydrophilic residues in this region. This particular mutation provides a useful test for this approach for analyzing PFIC/BRIC mutations, because the G1040R mutation in ATP8B1 has already been the subject of previous investigations. The results of these earlier experiments show that the mutated protein is relatively stable (37, 38). Although there is evidence that ATP8B1 harboring the G1040R mutation does not collect at the

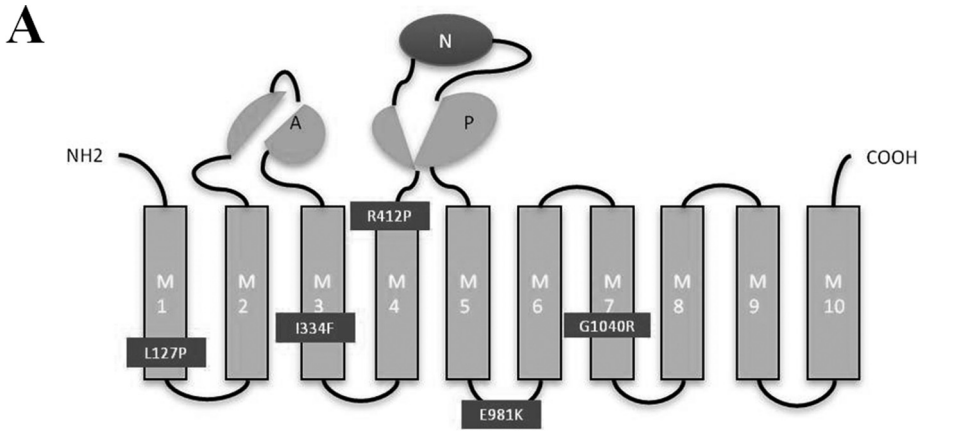

B

	L127	I334	R412	E981	G1040
ATP8B1	AANLYFLA**L**LILQAVFQ	LMNYMVYT**I**FVVLILLS	LYVSVEVI**R**LGQSHFIN	GYSAQTAY**E**DWFITLYN	RFFVSLLH**G**VLTSMILF
Dnf-2	FANIYFLI**L**LILGAFQI	ELNFSVIL**N**FVLLFILC	LYISVETT**K**TAQAIFIY	NFDGSYLF**E**YTYLTFYN	KFLWYMLD**G**VYQSVICF
3b8c	PLSWVMEM**A**AIMAIALA	VLTAIGNF**C**ICSIAIGM	MPTVLSVT**M**AIGSHRLS	EFDFS-----AFMVLII	VVLGGYQA**I**MTVIFFWA

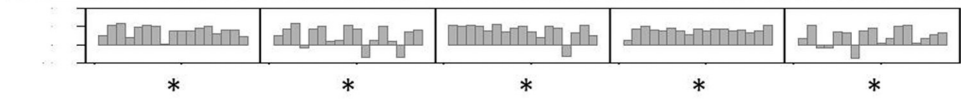

* * * * *

C

	ATP8B1	Dnf-2	38BC
PFIC	L127P	L264P	A76
BRIC	I334F	N601F	C247
PFIC	R412P	K670P	M297
PFIC	E981K	E1261K	S672-A673
PFIC	G1040R	G1320R	G717

FIGURE 3. *A*, locations of mutations tested here on a schematic of P4ATPase organization (phosphorylation (*P*), nucleotide binding (*N*), and actuator (*A*) domains are shown). *Dark boxes* show mutation in ATP8B1. *B*, local alignment of ATP8B1 and Dnf2p sequence around mutations. the bar graph *below* shows the conservation scores based on an alignment with ~250 P4-ATPase sequences. The conservation scores as determined by Consurf have been multiplied by −1 so that more positive values correspond to more conserved residues. *, mutated residue. *C*, corresponding residues in ATP8B1, Dnf2p, and the proton pump AHA2 structure (Protein Data Bank entry 3B8C).

canalicular membrane (37), it does reach the plasma membrane (38), although perhaps at reduced levels (37). It has been reported that this mutant protein may interact with its subunit from the Cdc50 family (38), although the interaction may be weak (37). Because there is no assay for transport by ATP8B1, these studies could not provide evidence one way or another on the crucial question of whether the mutation affects enzyme activity.

With this background, we investigated the properties of the corresponding Dnf2p mutant, G1320R. As in the case of the ATP8B1 mutant, we found that the mutated yeast protein is reasonably stable and accumulates in cells to concentrations comparable with those of the wild type protein expressed from the same promoter under the same conditions (Fig. 4). However, the mutated protein is completely incapable of transporting phospholipids (Fig. 5*A*). In addition, the ability of the G1320R mutant to interact with Lem3p, the normal subunit for this transporter, is also largely abrogated (Fig. 6). Together, these data show that, although this mutation does not have dramatic effects on protein stability, its disease phenotype is readily explained by its effect on protein activity.

L264P—The PFIC mutant L127P, corresponding to L264P in Dnf2p, was identified in a Japanese patient (10, 39) and substitutes a hydrophobic but helix-breaking proline for a moderately conserved leucine in the first transmembrane domain near the lumenal side of the membrane. This mutated ATP8B1 has also been the subject of experiments that suggested that the protein was stable, properly localized in the cell, and able to interact with its cognate Cdc50 family subunit (38), raising the question of why it results in disease. We therefore analyzed the homologous L264P mutant of Dnf2p. As in the case of the ATP8B1 homolog, the mutant is as stable as wild type enzyme (Fig. 4); moreover, as shown in Fig. 5*A*, it transports at the same maximal rate, and with the same K_m, as wild type enzyme, showing that the mutated enzyme is both active and properly localized. However, the interaction of the mutant Dnf2p with Lem3p is measurably weaker than that observed with the wild type transporter (Fig. 6), which may finally provide a clue as to why the corresponding ATP8B1 mutation has an abnormal phenotype in humans.

K670P—The R412P mutation in ATP8B1, corresponding to K670P in Dnf2p, was identified as a homozygous mutation in a

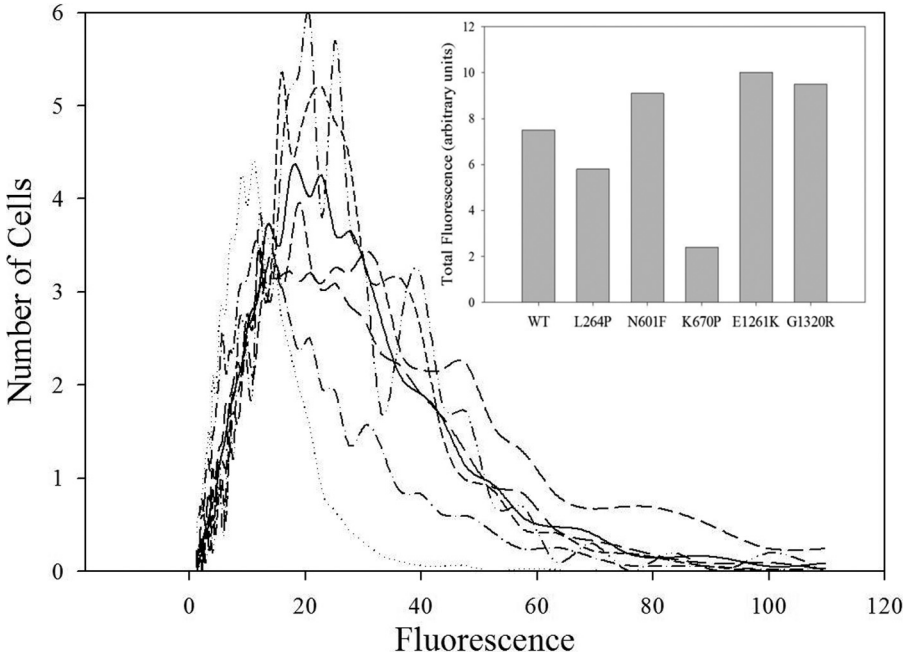

FIGURE 4. **Protein expression levels.** Binding of Alexa-tagged anti-HA antibody to a C-terminal HA-tagged Dnf2p was measured by cytometry. Curves are FITC fluorescence histograms for permeabilized cells, as judged by the ability to bind PI. . . . . ., no *dnf2*; ——, wild type *dnf2*; – – – -, L264P; - - - - -, N601F; –·–·–, K670P; – – – –, E1261K; –··–··, G1320R. *Inset*, total fluorescence over background. Total fluorescence was calculated by multiplying the fluorescence of each bin by the fraction of total cells in that bin, total fluorescence in the absence of *dnf2* was subtracted, and the remainder was shown to provide an estimate of the overall protein level.

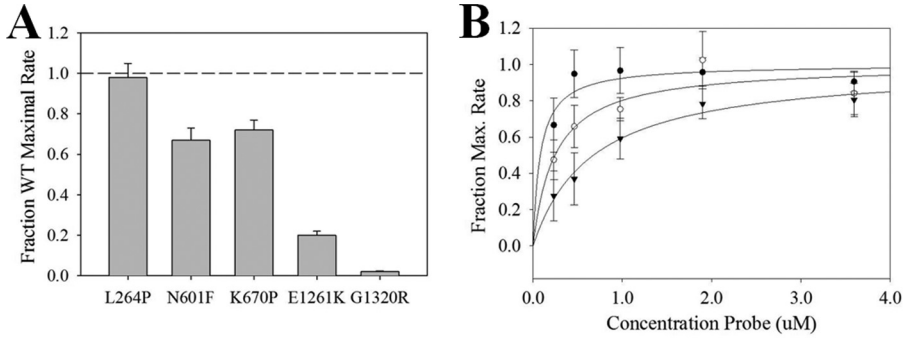

C

	Km (uM)	SE	Vmax Fraction of WT	SE
Wild Type	0.24	0.08	1	-
L264P	0.23	0.08	0.98	0.07
N601F	0.66	0.19	0.67	0.06
K670P	0.29	0.07	0.72	0.05
E1261K	0.08	0.04	0.20	0.02
G1320R	-	-	0.021	0.004

FIGURE 5. **Effect of PFIC BRIC mutations in *dnf2* on PC transport at the plasma membrane.** *A*, maximal transport rate for each of the PFIC/BRIC mutations in *dnf2* as a fraction of the rate observed in parallel with wild type *dnf2* control. *B*, apparent K_m measurement. The uptake rate as a function of NBD-PC concentration was measured for wild type (*open circles*), N601F (*filled triangles*), and E1261K (*filled circles*). The fraction of the maximal rate observed for each mutant (see Fig. 5*A*) was plotted against different concentrations of probe and fitted to the equation, $f = V_{max}/(1 + (K_m/x))$. At least two separate clones of each mutation were tested, and the results were averaged. *C*, summary of apparent K_m and V_{max} with S.E. values for each mutant *dnf2*. *Error bars*, S.E.

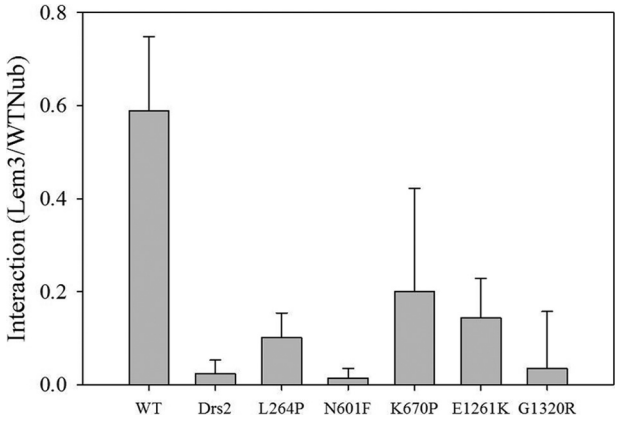

FIGURE 6. **Subunit transporter interaction.** Interaction was quantified by measuring β-galactosidase activity in extracts from diploid yeast containing Cub-tagged *dnf2*. Diploids containing a Nub fragment (*NubWT*) that does not require transporter/subunit interaction to associate with Cub fragments were used as a positive control for Cub-tagged transporter synthesis levels. Diploids containing an empty vector Nub plasmid were used to estimate background β-galactosidase levels for each mutant *dnf2*. Interaction was estimated in diploids containing Nub-tagged Lem3p. After subtraction of background from each, expression was calculated as the ratio of β-galactoside activity in the diploid containing Lem3p to that in the diploid containing the positive control Nub. The S.E. value (*error bars*) was calculated from measurements of the β-galactosidase activity in at least three independent diploids.

Japanese PFIC patient (10, 39). The affected residue is not, strictly speaking, in the transmembrane domain but rather is a conserved cationic residue (arginine or lysine) highly characteristic of the P4-ATPases and located on the cytoplasmic side of TM4 about two turns of the helix away from a tyrosine that is critical for determining headgroup specificity (25). The corresponding K670P mutation in Dnf2p appears to be less stable than the wild type enzyme, judging from the amount of protein present in the transformants (Fig. 4). In measurements of transport, the maximal rate of transport is correspondingly reduced, suggesting that although unstable, some protein does reach the plasma membrane and is functional there. As would be expected for a mutation outside the membrane region, the enzyme shows no significant difference in apparent K_m for substrate. Finally, Lem3p-dependent proteolytic release of the Cub tag from the transporter is also somewhat reduced, as would be expected if the amount of the Cub-tagged transporter in the cell is reduced.

N601F—The I334F mutation in ATP8B1, corresponding to the N601F mutation in Dnf2p, was originally identified in a compound heterozygosity with S453Y in a BRIC patient (10). This residue is moderately conserved in a class-specific fashion; it is a hydrophobic residue in the Drs2p/ATP8A1 class, including the ATP8B1 protein, whereas it is a well conserved asparagine in the Dnf1/2p class of transporters. It is located in approximately the middle of the membrane in TM3, which puts it near a lysine residue proposed as a potential substrate binding site in ATP8A2 (40). When the N601F equivalent mutation was introduced into Dnf2p, there was no effect on protein expression levels (Fig. 4) and, by extension, on protein stability. However, the mutation has a significant effect on the enzymatic properties of the transporter (Fig. 5). In the first place, the maximal rate of transport by this mutant was lower by about one-third than that of the wild type protein under identical conditions. More dramatically, the mutation resulted in a substantial increase in the apparent K_m for the substrate, corresponding to a reduced affinity for the phospholipid presented from the lumenal side of the membrane. Finally, the apparent affinity of the transporter for the Lem3p subunit in the split ubiquitin assay is much lower than that of the wild type enzyme (Fig. 6). These results show that this mutation, although it causes a relatively mild form of the disease, has readily measurable effects on transporter properties.

E1261K—The E981K mutation in ATP8B1, corresponding to an E1261K mutation in Dnf2p, was identified in a Japanese PFIC patient (41). The mutation changes a well conserved anionic residue in the lumenal loop between TM5 and TM6 to an equally but oppositely charged lysine residue. The change in the charge has no obvious effect on the stability of the protein (Fig. 4), which is present at the same levels as the wild type enzyme under the same circumstances. Despite this normal stability, the effect of the mutation on activity is dramatic, with the maximal activity reduced by almost 80% from that observed with wild type enzyme (Fig. 5). When the affinity of the enzyme for substrate was measured, the results were unexpected; the mutation resulted in a decrease in the apparent K_m for phospholipid, corresponding to an increase in affinity for the substrate. At the same time, there was a significant decrease in the interaction between the transporter and the Lem3p subunit. Together, these characteristics make the behavior of this mutation unique among all of the mutations studied here.

DISCUSSION

An Assay for Measuring P4-ATPase Activity—Understanding the biochemistry of phospholipid transport by P4-ATPases requires robust assays for their activity. By their nature, however, these assays present interesting problems. Although purified enzyme activity can readily be measured as ATP hydrolysis activity, this activity may be decoupled from transport. There have been interesting conclusions drawn from such assays (40, 42), but the presence of detergents and the absence of the bilayer make kinetic measurements difficult to interpret. Although very elegant experiments with reconstituted enzymes have also been useful (2, 3, 40), these experiments have also highlighted an important problem with this approach. In the small vesicles that result from reconstitution, only end point measurements are possible, because a single P4-ATPase molecule, with a k_{cat} on the order of 10^2/s (2, 43), can transport all of the relevant phospholipids in a time much too fast (a few s) to measure on the bench top. It should be noted that these considerations make it difficult to interpret transport measurements in vesicles that involve incubation times extending over large fractions of an hour or even longer.

The NBD-probe assay described in this study is a useful improvement in the ability to directly and quantitatively assay the phospholipid flipping activity of P4-ATPases. In exchange for the disadvantage of losing some measure of control over the experimental environment of the enzyme, the *in vivo* assay provides advantages of tractability and physiological relevance. The results make clear that, as should be the case, P4-ATPase-mediated transport of phospholipids from the outer leaflet is fast, on time scales best measured in seconds. Nevertheless, the

data also show that it is the transport step that is rate-limiting; the probe saturates external binding sites at a rate too fast for the assay to measure. The low level of PC transport observed when *dnf1* and *dnf2* are deleted shows that endocytic uptake of phospholipids is negligible under the conditions of the assay, a result that is not unexpected given the short duration of the uptake measurements and the low level of steady-state probe incorporation into the membrane (Fig. 1*D*). Although not exploited extensively in these studies, the data from the lyso-PC inhibition experiment show that a competition protocol can be used to obtain information about transported substrates whose uptake cannot be directly measured. Even this preliminary experiment, however, suggests that the P4-ATPases will act as lysophospholipid uptake enzymes when the concentrations of such potential substrates in the medium reach the micromolar level. Although in this case the affinity for the lysophospholipid is higher than for the corresponding phospholipid probe, these results do not show that uptake of such lysophospholipids is the primary function of these transporters, because it is known that NBD phospholipids may not be as efficiently taken up by P4-ATPases as natural phospholipids (44).

Insights about PFIC and BRIC—Several of the findings reported here tend to validate the strategy of analyzing PFIC mutants by studying the properties of the corresponding mutations in Dnf2p. The most useful of the evidence comes from those mutations that have already been subject to study in the human transporter. The unexpected stability of the protein molecule harboring the G1040R mutation (the reduced but still substantial protein levels), combined with a compromised interaction with subunit, are reflected faithfully in the phenotype of the G1320R mutant of Dnf2p. Similarly, the robust normality of the L127P mutant in ATP8B1 is reproduced in the L264P form of Dnf2p. So far as direct comparisons can be made, these data suggest that the evolutionary conservation of residues is consistent with a similarity in the phenotypes of the corresponding mutations in the two proteins.

The development of disease symptoms when ATP8B1 is mutated is strong evidence that the mutation has a significant impact on transporter function, even if the affected function is not known. In the absence of functional assays, the ability to measure protein synthesis has concentrated attention on possible indirect effects of such mutations (*e.g.* on protein folding) (16, 38). Indeed, the data presented here support just such a mechanism for the effect of the PFIC mutation R412P, where the corresponding K670P mutant shows parallel reductions in protein level, in maximal transport activity, and in transporter available for interaction with subunit, whereas the activity that remains seems normal in its affinity for phospholipid substrate.

In the mutations studied here, the phenotype of the R412P/K670P mutation is an outlier in that it has an impact on protein stability but little effect on the enzymatic properties of the transporter. That said, there is considerable diversity in the nature of the effects on phenotypes. The simplest of these is the phenotype of G1040R/G1320R, where the disruption of TM7 results in no transport activity at the plasma membrane and little interaction with subunit. Although less dramatic, both I334F/N601F and E981K/E1261K are also mutations that do not reduce protein levels but do reduce transport activity at the plasma membrane as well as interaction with subunit. Remarkably, the effects of these mutations on K_m are complete opposites of one another, a matter discussed in more detail below. The lack of effect of the L127P/L264P mutation on protein levels confirmed here is complemented by the lack of effect of this mutation on either maximal transport activity or substrate affinity, raising the question of why a patient harboring this mutation has PFIC at all. The observation of a reduced affinity for subunit observed with the L264P mutation may point to an explanation, especially in light of an important difference between the human and yeast systems. In yeast, each of the P4-ATPases, with the exception of Neo1p, is associated with its own subunit; in the case of Dnf2p, that subunit is Lem3p, a subunit that is shared with Dnf1p in normal yeast but is not shared in our experimental system because Dnf1p is not present. In humans, it is likely that all of the P4-ATPases interact with a common pool of subunits, because there are only three subunit genes in mammals, one of which is probably not functional (45), and 12 transporters other than the two ATP9 relatives of *neo1*. Under physiological conditions, the L127P mutant of ATP8B1 may thus be at a disadvantage in competition with other transporters for this common pool of subunits. Because association with a subunit is a functional necessity (6–8, 19), this disadvantage may be the source of the disease phenotype.

Together, these data show that each of the mutations originally identified in ATP8B1 results in a measurable defect when recreated in Dnf2p and, in most cases, in a defect in the level of transport activity at the physiologically relevant location. Because so much less is known with certainty about the properties of ATP8B1, these results are probably best treated as qualitative indications of the nature of the induced defects rather than quantitative predictions of the phenotypes of the corresponding ATP8B1 forms. For example, the results of Baldridge and Graham (25) suggest that the same residue is important in two transporters (Drs2p and Dnf1p) with different transport specificities. However, the collection of residues that interact with substrate is undoubtedly larger than the list that is already known. As a result, until the specificity and kinetic parameters of phospholipid binding and transport are directly characterized and quantitated for ATP8B1 itself, the changes in PC transport measured here can only provide an indication of the kind of defect that these mutations induce. Nevertheless, even this information clearly differentiates between the consequences of different mutations, making these results a potentially useful guide to how different forms of the disease might be understood and treated.

In thinking about the more general implications of the phenotypes of these mutations, and particularly their effects on interaction between subunit and transporter, it is important to remember that the latter is not static; quite to the contrary, it is a dynamic part of the reaction cycle of transport (6). In particular, the subunit interacts most strongly with the lumenal-facing E2P conformation of the enzyme, the point where the transporter binds the phospholipid substrate. Mutations can affect subunit-transporter interaction, not by directly altering the protein-protein interaction between the two peptides, but by altering the rates of individual steps in the reaction cycle, and

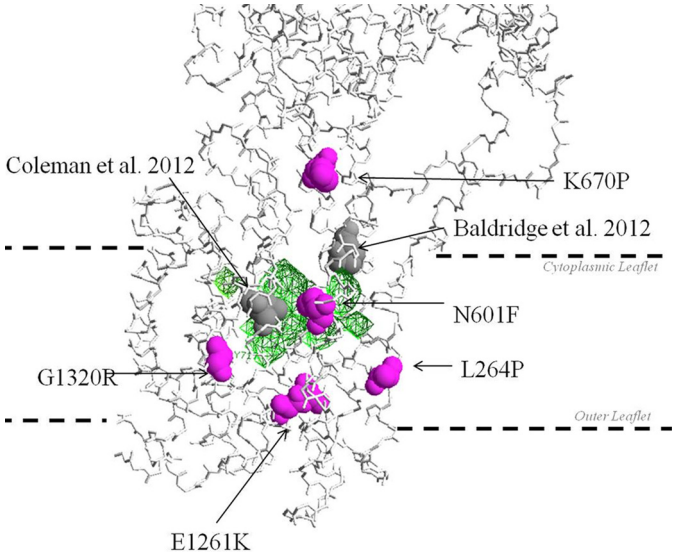

FIGURE 7. **Locations of mutated residues mapped on the crystal structure of the proton pump AHA2 (Protein Data Bank entry 3B8C).** The location of key PFIC/BRIC mutants studied are shown in a *magenta space-filling representation* for the corresponding residues in the proton pump structure (see Fig. 3*C*). Functionally important residues identified by others are shown in a *gray space-filling representation* to facilitate comparison. The location of the water-filled cavity in the proton pump cycle is rendered in *green*. Important residues from previous studies are rendered in a *gray space-filling representation* and *labeled* accordingly. The predicted location of the plasma membrane is shown by the *dashed lines*.

thereby how the protein is distributed between different conformational stages of the reaction cycle. One consequence of this complex dynamic is that the relationship between interaction and transport activity is not readily predictable, as has been observed in the study of subunits with altered disulfides in the lumenal domain (46).

Recently, a conserved tyrosine on the cytoplasmic surface of the transmembrane region was shown to be an important determinant of the substrate specificity of transport (25). This work provided direct experimental support for an earlier conjecture for the existence of such a cytoplasmic binding site (47) based on high resolution structural studies of the E2 form of the sarcoplasmic reticulum Ca^{2+}-ATPase (48). These ideas suggest that phospholipid transport involves two phospholipid binding sites on opposite sides of the membrane, with a pathway for headgroup diffusion that links them (49). This model may help explain the two mutations studied here, I334F/N601F and E981K/E1231K, which both slow the rate of transport but have opposite effects on substrate affinity. The first of these alters a residue that is a neighbor in the overall structure of the lysine studied by Coleman *et al.* (40). Substitution of an alanine for that residue, like the BRIC substitution I334F, reduces apparent affinity for the phospholipid substrate and, as shown here, reduces the transport rate. It has been noted previously that the conserved lysine points toward the center of the transmembrane region. When the P4-ATPase sequence is aligned to the known crystal structure of the proton pump (Protein Data Bank entry 3B8C), the lysine faces the water-filled pocket, which allows proton exchange with the lumenal surface (Fig. 7). The N601F mutation also corresponds to a residue that borders this pocket, consistent with the view that the similarity in their phenotype is a reflection of their proximity in the structure. The results here add another piece of information; the mutation dramatically reduces the apparent affinity of the transporter for the subunit. Because the altered residues in these cases are inside the transporter, it seems unlikely that these residues are at the transporter/subunit interface. A more likely explanation is that mutation of these residues makes it more difficult for the enzyme to adopt the so-called ADP-insensitive E2P conformation. In this form of the enzyme, the substrate is occluded and exchanging between the two sides of the bilayer (40), and the transporter has a high affinity for the subunit (6). Mutations that make it difficult for the enzyme to adopt this occluded conformation may depopulate it and thereby reduce the apparent affinity of the enzyme for the cognate subunit.

In this regard, the E981K/E1231K mutation addresses an important issue. In well known P-type ATPases, there is a single binding site in the center of the bilayer into which substrates diffuse from the outer leaflet at one stage of the reaction cycle and from which they diffuse into the inner leaflet at another stage. The binding site of Baldridge and Graham (25) on the cytoplasmic surface, because of its location, cannot contribute to the affinity of the enzyme for phospholipids presented from the lumenal side of the bilayer. Importantly, there has never been any evidence pointing to where phospholipid might enter from the lumenal surface of the bilayer. The mutated glutamate in the E981K/E1231K mutants is unambiguously on the lumenal surface, in a loop that is not present in the ion or proton transporters. The increase in the apparent affinity of the transporter for the probe in this mutant suggests that it has a lumenal binding site for phospholipid or near this loop. Because this residue is on an insertion that is not present in the proton transporter, locating it in the 3B8C structure data is necessarily inaccurate. Even so, it can be seen (Fig. 7) that the region of the proton transporter where the P4-ATPase insertion appears is in relatively close proximity to an opening to the water binding pocket. The properties of this particular mutation are also interesting because of the dramatic decrease in transport associated with its increase in substrate affinity. Increasing the affinity of the lumenal site for the substrate will tend to depopulate enzyme conformations with phospholipid on the cytoplasmic side and thus slow the rate of transport.

The wide distribution of locations of residues important for phospholipid translocation across the transmembrane region is consistent with a requirement for large scale substrate movement through enzyme during sequential phases of the reaction cycle (49). The yeast platform and NBD-probe uptake assay provide powerful tools for the study of new PFIC/BRIC mutations as they emerge, and the study of such mutations provides new hints for identifying residues that are important for substrate movement and perhaps even for predicting their contribution to enzyme activity.

REFERENCES

1. Tang, X., Halleck, M. S., Schlegel, R. A., and Williamson, P. (1996) A subfamily of P-type ATPases with aminophospholipid transporting activity. *Science* **272,** 1495–1497
2. Coleman, J. A., Kwok, M. C., and Molday, R. S. (2009) Localization, purification, and functional reconstitution of the P4-ATPase Atp8a2, a phosphatidylserine flippase in photoreceptor disc membranes. *J. Biol. Chem.* **284,** 32670–32679

3. Zhou, X., and Graham, T. R. (2009) Reconstitution of phospholipid translocase activity with purified Drs2p, a type-IV P-type ATPase from budding yeast. *Proc. Natl. Acad. Sci. U.S.A.* **106,** 16586–16591
4. Axelsen, K. B., and Palmgren, M. G. (2001) Inventory of the superfamily of P-type ion pumps in *Arabidopsis*. *Plant Physiol.* **126,** 696–706
5. Saito, K., Fujimura-Kamada, K., Furuta, N., Kato, U., Umeda, M., and Tanaka, K. (2004) Cdc50p, a protein required for polarized growth, associates with the Drs2p P-type ATPase implicated in phospholipid translocation in *Saccharomyces cerevisiae*. *Mol. Biol. Cell* **15,** 3418–3432
6. Lenoir, G., Williamson, P., Puts, C. F., and Holthuis, J. C. (2009) Cdc50p plays a vital role in the ATPase reaction cycle of the putative aminophospholipid transporter Drs2p. *J. Biol. Chem.* **284,** 17956–17967
7. Bryde, S., Hennrich, H., Verhulst, P. M., Devaux, P. F., Lenoir, G., and Holthuis, J. C. (2010) CDC50 proteins are critical components of the human class-1 P4-ATPase transport machinery. *J. Biol. Chem.* **285,** 40562–40572
8. Coleman, J. A., and Molday, R. S. (2011) Critical role of the β-subunit CDC50A in the stable expression, assembly, subcellular localization, and lipid transport activity of the P4-ATPase ATP8A2. *J. Biol. Chem.* **286,** 17205–17216
9. Bull, L. N., van Eijk, M. J., Pawlikowska, L., DeYoung, J. A., Juijn, J. A., Liao, M., Klomp, L. W., Lomri, N., Berger, R., Scharschmidt, B. F., Knisely, A. S., Houwen, R. H., and Freimer, N. B. (1998) A gene encoding a P-type ATPase mutated in two forms of hereditary cholestasis. *Nat. Genet.* **18,** 219–224
10. Klomp, L. W., Vargas, J. C., van Mil, S. W., Pawlikowska, L., Strautnieks, S. S., van Eijk, M. J., Juijn, J. A., Pabón-Peña, C., Smith, L. B., DeYoung, J. A., Byrne, J. A., Gombert, J., van der Brugge, G., Berger, R., Jankowska, I., Pawlowska, J., Villa, E., Knisely, A. S., Thompson, R. J., Freimer, N. B., Houwen, R. H., and Bull, L. N. (2004) Characterization of mutations in ATP8B1 associated with hereditary cholestasis. *Hepatology* **40,** 27–38
11. Eppens, E. F., van Mil, S. W., de Vree, J. M., Mok, K. S., Juijn, J. A., Elferink, R., Berger, R., Houwen, R. H., and Klomp, L. W. (2001) FIC1, the protein affected in two forms of hereditary cholestasis, is localized in the cholangiocyte and the canalicular membrane of the hepatocyte. *J. Hepatol.* **35,** 436–443
12. Stapelbroek, J. M., Peters, T. A., van Beurden, D. H., Curfs, J. H., Joosten, A., Beynon, A. J., van Leeuwen, B. M., van der Velden, L. M., Bull, L., Oude Elferink, R. P., van Zanten, B. A., Klomp, L. W., and Houwen, R. H. (2009) ATP8B1 is essential for maintaining normal hearing. *Proc. Natl. Acad. Sci. U.S.A.* **106,** 9709–9714
13. Palmgren, M. G., and Nissen, P. (2011) P-type ATPases. *Annu. Rev. Biophys.* **40,** 243–266
14. Paulusma, C. C., Groen, A., Kunne, C., Ho-Mok, K. S., Spijkerboer, A. L., Rudi de Waart, D., Hoek, F. J., Vreeling, H., Hoeben, K. A., van Marle, J., Pawlikowska, L., Bull, L. N., Hofmann, A. F., Knisely, A. S., and Oude Elferink, R. P. (2006) Atp8b1 deficiency in mice reduces resistance of the canalicular membrane to hydrophobic bile salts and impairs bile salt transport. *Hepatology* **44,** 195–204
15. Paulusma, C. C., Folmer, D. E., Ho-Mok, K. S., de Waart, D. R., Hilarius, P. M., Verhoeven, A. J., and Oude Elferink, R. P. (2008) ATP8B1 requires an accessory protein for endoplasmic reticulum exit and plasma membrane lipid flippase activity. *Hepatology* **47,** 268–278
16. Verhulst, P. M., van der Velden, L. M., Oorschot, V., van Faassen, E. E., Klumperman, J., Houwen, R. H., Pomorski, T. G., Holthuis, J. C., and Klomp, L. W. (2010) A flippase-independent function of ATP8B1, the protein affected in familial intrahepatic cholestasis type 1, is required for apical protein expression and microvillus formation in polarized epithelial cells. *Hepatology* **51,** 2049–2060
17. Chen, C. Y., Ingram, M. F., Rosal, P. H., and Graham, T. R. (1999) Role for Drs2p, a P-type ATPase and potential aminophospholipid translocase, in yeast late Golgi function. *J. Cell Biol.* **147,** 1223–1236
18. Hua, Z., Fatheddin, P., and Graham, T. R. (2002) An essential subfamily of Drs2p-related P-type ATPases is required for protein trafficking between Golgi complex and endosomal/vacuolar system. *Mol. Biol. Cell* **13,** 3162–3177
19. van der Velden, L. M., Wichers, C. G., van Breevoort, A. E., Coleman, J. A., Molday, R. S., Berger, R., Klomp, L. W., and van de Graaf, S. F. (2010) Heteromeric interactions required for abundance and subcellular localization of human CDC50 proteins and class 1 P4-ATPases. *J. Biol. Chem.* **285,** 40088–40096
20. Pomorski, T., Lombardi, R., Riezman, H., Devaux, P. F., van Meer, G., and Holthuis, J. C. (2003) Drs2p-related P-type ATPases Dnf1p and Dnf2p are required for phospholipid translocation across the yeast plasma membrane and serve a role in endocytosis. *Mol. Biol. Cell* **14,** 1240–1254
21. Natarajan, P., Wang, J., Hua, Z., and Graham, T. R. (2004) Drs2p-coupled aminophospholipid translocase activity in yeast Golgi membranes and relationship to *in vivo* function. *Proc. Natl. Acad. Sci. U.S.A.* **101,** 10614–10619
22. Alder-Baerens, N., Lisman, Q., Luong, L., Pomorski, T., and Holthuis, J. C. (2006) Loss of P4 ATPases Drs2p and Dnf3p disrupts aminophospholipid transport and asymmetry in yeast post-Golgi secretory vesicles. *Mol. Biol. Cell* **17,** 1632–1642
23. Chen, S., Wang, J., Muthusamy, B. P., Liu, K., Zare, S., Andersen, R. J., and Graham, T. R. (2006) Roles for the Drs2p-Cdc50p complex in protein transport and phosphatidylserine asymmetry of the yeast plasma membrane. *Traffic* **7,** 1503–1517
24. Ling, M. M., and Robinson, B. H. (1997) Approaches to DNA mutagenesis. An overview. *Anal. Biochem.* **254,** 157–178
25. Baldridge, R. D., and Graham, T. R. (2012) Identification of residues defining phospholipid flippase substrate specificity of type IV P-type ATPases. *Proc. Natl. Acad. Sci. U.S.A.* **109,** E290–E298
26. Obrdlik, P., El-Bakkoury, M., Hamacher, T., Cappellaro, C., Vilarino, C., Fleischer, C., Ellerbrok, H., Kamuzinzi, R., Ledent, V., Blaudez, D., Sanders, D., Revuelta, J. L., Boles, E., André, B., and Frommer, W. B. (2004) K^+ channel interactions detected by a genetic system optimized for systematic studies of membrane protein interactions. *Proc. Natl. Acad. Sci. U.S.A.* **101,** 12242–12247
27. Grefen, C., Obrdlik, P., and Harter, K. (2009) The determination of protein-protein interactions by the mating-based split-ubiquitin system (mbSUS). *Methods Mol. Biol.* **479,** 217–233
28. Kakkar, T., Boxenbaum, H., and Mayersohn, M. (1999) Estimation of K_i in a competitive enzyme-inhibition model. Comparisons among three methods of data analysis. *Drug Metab. Dispos.* **27,** 756–762
29. Grefen, C., Lalonde, S., and Obrdlik, P. (2007) Split-ubiquitin system for identifying protein-protein interactions in membrane and full-length proteins. *Curr. Protoc. Neurosci.* Chapter 5, Unit 5.27
30. Pedersen, B. P., Buch-Pedersen, M. J., Morth, J. P., Palmgren, M. G., and Nissen, P. (2007) Crystal structure of the plasma membrane proton pump. *Nature* **450,** 1111–1114
31. Pei, J., Kim, B. H., and Grishin, N. V. (2008) PROMALS3D. A tool for multiple protein sequence and structure alignments. *Nucleic Acids Res.* **36,** 2295–2300
32. Ashkenazy, H., Erez, E., Martz, E., Pupko, T., and Ben-Tal, N. (2010) ConSurf 2010. Calculating evolutionary conservation in sequence and structure of proteins and nucleic acids. *Nucleic Acids Res.* **38,** W529–W533
33. McIntyre, J. C., and Sleight, R. G. (1991) Fluorescence assay for phospholipid membrane asymmetry. *Biochemistry* **30,** 11819–11827
34. Seigneuret, M., and Devaux, P. F. (1984) ATP-dependent asymmetric distribution of spin-labeled phospholipids in the erythrocyte membrane. Relation to shape changes. *Proc. Natl. Acad. Sci. U.S.A.* **81,** 3751–3755
35. Mukerjee, P., and Mysels, K. J. (1971) *Critical Micelle Concentrations of Aqueous Surfactant Systems*, United States National Bureau of Standards, Washington, D. C.
36. Riekhof, W. R., and Voelker, D. R. (2009) The yeast plasma membrane P4-ATPases are major transporters for lysophospholipids. *Biochim. Biophys. Acta* **1791,** 620–627
37. Folmer, D. E., van der Mark, V. A., Ho-Mok, K. S., Oude Elferink, R. P., and Paulusma, C. C. (2009) Differential effects of progressive familial intrahepatic cholestasis type 1 and benign recurrent intrahepatic cholestasis type 1 mutations on canalicular localization of ATP8B1. *Hepatology* **50,** 1597–1605
38. van der Velden, L. M., Stapelbroek, J. M., Krieger, E., van den Berghe, P. V., Berger, R., Verhulst, P. M., Holthuis, J. C., Houwen, R. H., Klomp, L. W., and van de Graaf, S. F. (2010) Folding defects in P-type ATP 8B1 associated with hereditary cholestasis are ameliorated by 4-phenylbutyrate.

Hepatology **51,** 286–296
39. Egawa, H., Yorifuji, T., Sumazaki, R., Kimura, A., Hasegawa, M., and Tanaka, K. (2002) Intractable diarrhea after liver transplantation for Byler's disease: successful treatment with bile adsorptive resin. *Liver Transpl.* **8,** 714–716
40. Coleman, J. A., Vestergaard, A. L., Molday, R. S., Vilsen, B., and Peter Andersen, J. (2012) Critical role of a transmembrane lysine in aminophospholipid transport by mammalian photoreceptor P4-ATPase ATP8A2. *Proc. Natl. Acad. Sci. U.S.A.* **109,** 1449–1454
41. Numakura, C., Abukawa, D., Kimura, T., Tanabe, S., and Hayasaka, K. (2011) A case of progressive familial intrahepatic cholestasis type 1 with compound heterozygous mutations of *ATP8B1*. *Pediatr. Int.* **53,** 107–110
42. Paterson, J. K., Renkema, K., Burden, L., Halleck, M. S., Schlegel, R. A., Williamson, P., and Daleke, D. L. (2006) Lipid specific activation of the murine P4-ATPase Atp8a1 (ATPase II). *Biochemistry.* **45,** 5367–5376
43. Moriyama, Y., and Nelson, N. (1988) Purification and properties of a vanadate- and *N*-ethylmaleimide-sensitive ATPase from chromaffin granule membranes. *J. Biol. Chem.* **263,** 8521–8527
44. Pomorski, T., Muller, P., Zimmermann, B., Burger, K., Devaux, P. F., and Herrmann, A. (1996) Transbilayer movement of fluorescent and spin-labeled phospholipids in the plasma membrane of human fibroblasts. A quantitative approach. *J. Cell Sci.* **109,** 687–698
45. Katoh, Y., and Katoh, M. (2004) Identification and characterization of *CDC50A*, *CDC50B* and *CDC50C* genes *in silico*. *Oncol. Rep.* **12,** 939–943
46. Puts, C. F., Panatala, R., Hennrich, H., Tsareva, A., Williamson, P., and Holthuis, J. C. (2012) Mapping functional interactions in a heterodimeric phospholipid pump. *J. Biol. Chem.* **287,** 30529–30540
47. Lenoir, G., Williamson, P., and Holthuis, J. C. (2007) On the origin of lipid asymmetry. The flip side of ion transport. *Curr. Opin. Chem. Biol.* **11,** 654–661
48. Obara, K., Miyashita, N., Xu, C., Toyoshima, I., Sugita, Y., Inesi, G., and Toyoshima, C. (2005) Structural role of countertransport revealed in Ca^{2+} pump crystal structure in the absence of Ca^{2+}. *Proc. Natl. Acad. Sci. U.S.A.* **102,** 14489–14496
49. Stone, A., and Williamson, P. (2012) Outside of the box: Recent News about Phospholipid translocation by P4 ATPases. *J. Chem. Biol.* **5,** 131–136
50. Robinson, J. S., Klionsky, D. J., Banta, L. M., and Emr, S. D. (1988) Protein sorting in *Saccharomyces cerevisiae*. Isolation of mutants defective in the delivery and processing of multiple vacuolar hydrolases. *Mol. Cell Biol.* **8,** 4936–4948
51. Maddock, J. R., Weidenhammer, E. M., Adams, C. C., Lunz, R. L., and Woolford, J. L., Jr. (1994) Extragenic suppressors of *Saccharomyces cerevisiae* prp4 mutations identify a negative regulator of PRP genes. *Genetics* **136,** 833–847